J Therm Anal Calorim (2016) 123:371–376
DOI 10.1007/s10973-015-4865-9

Structural and thermodynamic properties of Tutton salt $K_2Zn(SO_4)_2{\cdot}6H_2O$

Ae Ran Lim[1,2] · Sun Ha Kim[3]

Received: 23 January 2015 / Accepted: 13 June 2015 / Published online: 23 July 2015

Abstract The structural and thermodynamic properties of Tutton salt $K_2Zn(SO_4)_2{\cdot}6H_2O$ were investigated using thermogravimetric analysis, differential scanning calorimetry, and nuclear magnetic resonance. The first mass loss of H_2O occurred around 353 K, which was interpreted as the onset of partial thermal decomposition, and the mass loss continues from T_d to 440 K. The temperature dependences of the spin–lattice relaxation time for the ^1H and ^{39}K nuclei were measured in the laboratory frame and in the rotating frame. The results were compared with those obtained for the series of compounds, i.e., $M_2Zn(SO_4)_2{\cdot}6H_2O$ (M = Na, Rb, and Cs), that were previously reported.

Keywords Tutton salts · $K_2Zn(SO_4)_2{\cdot}6H_2O$ · Structural property · Thermodynamic property · NMR · MAS NMR · Solid NMR · Phase transition

Introduction

Some inorganic salt hydrates have optimal melting temperatures and high enthalpies of fusion and are thus suitable for storing the energy absorbed by solar collectors [1, 2]. For domestic heating and hot-water supplies, this energy might be stored chemically in the form of reversible reactions, thermally in the form of phase changes, or as temperature increases in the storage material. Therefore, further studies of the physical properties of salt hydrates are needed, in particular, to obtain precise structural information for metal–water bonded systems [2]. Tutton salts are an isomorphous series of monoclinic crystals with the general formula $M^I_2M^{II}(SO_4)_2{\cdot}6H_2O$. They contain two octahedral hexahydrate complexes $[M^{II}(H_2O)_6]^{2+}$ in the crystal unit cell, where M^{II} is a divalent cation (Co, Zn, Fe, or an ion of the 3*d* group), and M^I is a monovalent cation (Na, K, Rb, or Cs) [3–11]. The unit cell dimensions and molecular structures of the crystals of this family are very similar. Montgomery and Lingafelter [12] described the structural characteristics of the crystals in this series, including the details of their hydrogen bond networks. One $M_2Zn(SO_4)_2{\cdot}6H_2O$ compound, $K_2Zn(SO_4)_2{\cdot}6H_2O$, has a monoclinic structure with space group $P2_1/a$. The unit cell contains two Zn^{2+} ions, each surrounded by six water molecules forming an octahedron, as shown in Fig. 1. $K_2Zn(SO_4)_2{\cdot}6H_2O$ is composed of $Zn(H_2O)_6$ octahedra and SO_4 square planar forms. The $Zn(H_2O)_6$ octahedral form is highly distorted, as indicated by the Zn–O bond. Each $[Zn(H_2O)_6]^{2+}$ complex cation is surrounded by four sulfate anion acceptor groups and four K cation donor groups.

The purpose of this study was to investigate the structural and thermodynamic properties of $K_2Zn(SO_4)_2{\cdot}6H_2O$ single crystals using differential scanning calorimetry (DSC) and thermogravimetric analysis (TG). In addition, the temperature dependence of the spin–lattice relaxation time in the laboratory frame, T_1, and the spin–lattice relaxation time in the rotating frame, $T_{1\rho}$, for the ^1H and ^{39}K nuclei in $K_2Zn(SO_4)_2{\cdot}6H_2O$ was investigated using a pulse nuclear magnetic resonance (NMR) spectrometer to obtain detailed information about the physical properties. This was the first investigation of the structural changes in

✉ Ae Ran Lim
aeranlim@hanmail.net; arlim@jj.ac.kr

[1] Department of Science Education, Jeonju University, Jeonju 560-759, South Korea

[2] Department of Carbon Fusion Engineering, Jeonju University, Jeonju 560-759, South Korea

[3] Korea Basic Science Institute Seoul Western Center, Seoul 120-140, South Korea

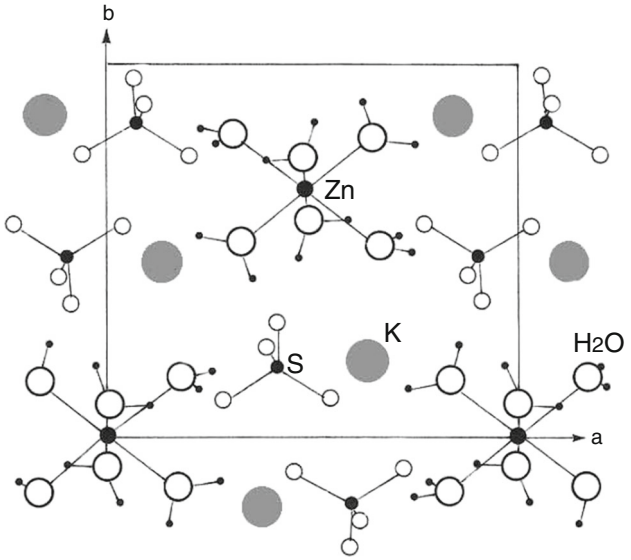

Fig. 1 Crystal structure of $K_2Zn(SO_4)_2{\cdot}6H_2O$ projected onto the *ab* plane

$K_2Zn(SO_4)_2{\cdot}6H_2O$ crystals. We used the results to analyze the environments of their ^1H and ^{39}K nuclei. We also compared our results to those obtained with $Na_2Zn(SO_4)_2{\cdot}6H_2O$, $Rb_2Zn(SO_4)_2{\cdot}6H_2O$, and $Cs_2Zn(SO_4)_2{\cdot}6H_2O$, which have been reported previously. Further studies of the physical properties of salt hydrates are needed, in particular, to obtain precise structural information for metal–water bonded systems.

Experimental method

Single crystals of $K_2Zn(SO_4)_2{\cdot}6H_2O$ were grown by slow evaporation from an aqueous solution at 293 K. The resulting single crystals were colorless and transparent with dimensions 4 × 6 × 3 mm.

The NMR spectrum of the ^1H and ^{39}K nuclei for the $K_2Zn(SO_4)_2{\cdot}6H_2O$ single crystals in the laboratory frame was measured by using the Varian 200 FT NMR and Bruker 400 FT NMR spectrometers at the Korea Basic Science Institute Seoul Western Center. The central radio frequency was set at $\omega_0/2\pi = 200$ MHz for the ^1H nucleus and $\omega_0/2\pi = 18.67$ MHz for the ^{39}K nucleus. A probehead with a solenoid coil was used. The spin–lattice relaxation time in the laboratory frame T_1 was measured by applying the pulse sequences π–t-$\pi/2$-acquisition for ^1H and $\pi/2$–t–$\pi/2$-acquisition for ^{39}K. The nuclear magnetizations $S(t)$ of the ^1H nucleus at time t after the π pulse were determined from the saturation recovery sequence following the pulse, whereas those of the ^{39}K nucleus at time t after the $\pi/2$ pulse were determined from the inversion recovery sequence following the pulse. The width of the $\pi/2$ pulse was 3.1 μs for ^1H and 33.3 μs for ^{39}K.

The ^1H magic angle spinning (MAS) NMR experiments in the rotating frame were also performed using the Varian 200 FT NMR and Bruker 400 FT NMR spectrometers at the Korea Basic Science Institute. The magnetic fields were 4.7 T and 9.4 T, and the ^1H MAS NMR experiments were performed at the Larmor frequencies of $\omega_0/2\pi = 200$ MHz and $\omega_0/2\pi = 400$ MHz, respectively. A MAS probehead with a 4-mm zirconia rotor was used. The MAS rate was set to 10 kHz to minimize spinning sideband overlap. The spin–lattice relaxation times in the rotating frame $T_{1\rho}$ were measured by varying the duration of a spin-locking pulse applied after a direct polarization of spins, i.e., $\pi/2$—spin lock-acquisition. The width of the $\pi/2$ pulse was 3 μs for ^1H at $\omega_0/2\pi = 200$ MHz and 5 μs for ^1H at $\omega_0/2\pi = 400$ MHz. The temperature-dependent NMR measurements were obtained over the temperature range of 180–420 K. The samples were maintained at constant temperatures by controlling the flow of nitrogen gas and the heater current.

The crystal structure of $K_2Zn(SO_4)_2{\cdot}6H_2O$ was determined using an X-ray diffractometer system with Bruker AXS GMBH at the Korea Basic Science Institute Western Seoul Center. The crystal was mounted on a Bruker SMART CCD diffractometer equipped with a graphite-monochromated Mo Kα radiation source ($\lambda = 0.71073$ Å). Data collection and integration were performed with SMART (Bruker 2000) and SAINT-Plus (Bruker 2001) [13]. The structure of the $K_2Zn(SO_4)_2{\cdot}6H_2O$ crystals at room temperature exhibits monoclinic symmetry with cell parameters $a = 9.041$ Å, $b = 12.310$ Å, $c = 6.182$ Å, $\alpha = \gamma = 90°$, and $\beta = 104.777°$. These results are consistent with the data of Montgomery and Lingafelter [12]. In addition, the phase transition temperatures of the crystals were determined by DSC measurements with a DuPont 2010 DSC instrument at a heating rate of 10 °C min^{-1}. Two endothermic peaks were observed at 386 and 410 K, as shown in Fig. 2. TG was then used to determine whether these high-temperature transformations are structural phase transitions or chemical reactions. The curve of $K_2Zn(SO_4)_2{\cdot}6H_2O$ is shown in Fig. 3. The first mass loss begins around 353 K and reaches 4 and 16 % for $K_2Zn(SO_4)_2{\cdot}5H_2O$ and $K_2Zn(SO_4)_2{\cdot}2H_2O$, respectively. Near 438 K, the thermal decomposition enters a new stage, and the residue of the final products reaches a value of 75.64 %, along with the escape of H_2O. The bulk mass of $K_2Zn(SO_4)_2{\cdot}6H_2O$ decreases at 353 K (T_d) and reaches complete thermal decomposition into $K_2Zn(SO_4)_2$ around 438 K. In TG of Fig. 3, the mass loss continues from T_d to 440 K at a heating rate of 10 °C min^{-1}. The DSC, TG, and optical polarizing microscopy results for $K_2Zn(SO_4)_2{\cdot}6H_2O$ crystals show that the mass loss around 353 K ($=T_d$) is due to the onset of partial thermal decomposition. The two endothermic peaks at 386 and 410 K in DSC are not

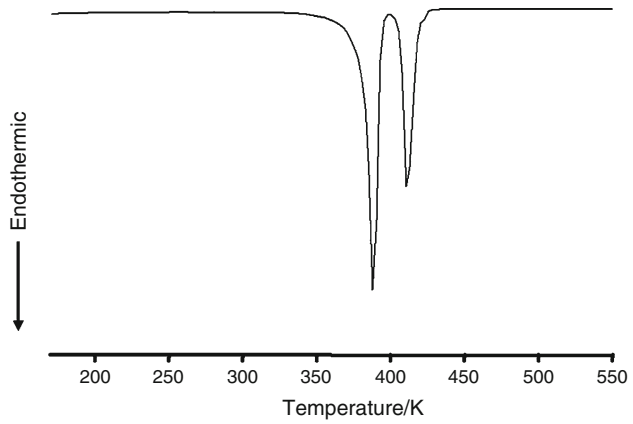

Fig. 2 DSC curve of $K_2Zn(SO_4)_2{\cdot}6H_2O$

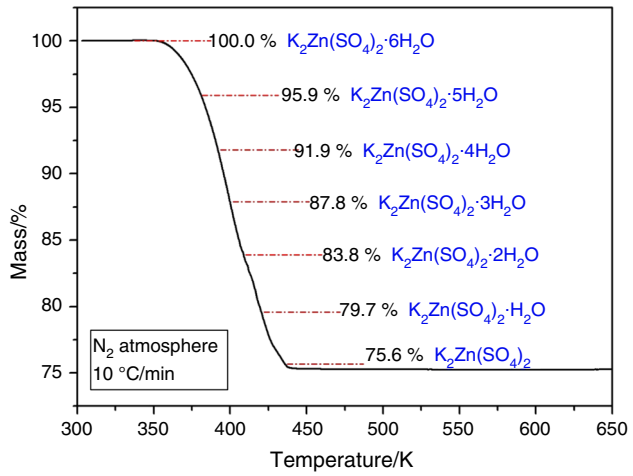

Fig. 3 Thermogravimetric analysis (TG) of $K_2Zn(SO_4)_2{\cdot}6H_2O$

polymorphic phase transitions but dehydration accompanied by loss of H_2O.

Experimental results and discussion

Spin–lattice relaxation time for ^{1}H of $K_2Zn(SO_4)_2{\cdot}6H_2O$ in the laboratory and rotating frames

The values for ^{1}H spin–lattice relaxation time in the laboratory frame T_1 were obtained by a static NMR method at a frequency of 200 MHz. The saturation recovery traces of the magnetizations for ^{1}H in $K_2Zn(SO_4)_2{\cdot}6H_2O$ crystals were determined at several different temperatures. The relaxation time was then determined directly from the slope of each log $[S(\infty) - S(t)]/S(\infty)$ versus t plot [14]. The temperature dependence of T_1 for ^{1}H is shown in Fig. 4; T_1 decreases with increasing temperature. The T_1 values for ^{1}H are more or less continuous near T_d.

A structural analysis of ^{1}H in $K_2Zn(SO_4)_2{\cdot}6H_2O$ was conducted using MAS NMR experiments at two different Larmor frequencies, 200 MHz and 400 MHz. The ^{1}H MAS NMR spectrum of a $K_2Zn(SO_4)_2{\cdot}6H_2O$ crystal at 300 K is shown in Fig. 5. The spectrum consists of one peak at a chemical shift of $\delta = 6.49$ ppm; this signal is attributed to water protons. The spinning sidebands are marked with asterisks. The values of the spin–lattice relaxation times in the rotating frame $T_{1\rho}$ were obtained for the protons in $K_2Zn(SO_4)_2{\cdot}6H_2O$ by MAS NMR experiments at several temperatures. The nuclear magnetization recovery traces obtained for the protons have been described by the following single exponential function,

$$S(t) = S(0)\exp\left(-t/T_{1\rho}\right), \quad (1)$$

where $S(t)$ is the magnetization at delay time t, and $S(0)$ is the total nuclear magnetization of ^{1}H at thermal equilibrium [15]. The recovery traces showed single exponential decay at all temperatures. The temperature dependence of $T_{1\rho}$ for ^{1}H is shown in Fig. 4. The slope of the proton $T_{1\rho}$ data changes abruptly near T_d. As mentioned above, this temperature is associated with the onset of partial thermal decomposition. The variation of $T_{1\rho}$ with temperature exhibits a minimum: 7.15 ms at 230 K for 200 MHz and 9.64 ms at 220 K for 400 MHz. This behavior of $T_{1\rho}$ indicates that a distinct molecular motion is present. The minimum temperature is different in each case owing to the Larmor frequency; $T_{1\rho}$ depends on the frequency.

Spin–lattice relaxation time for ^{39}K of $K_2Zn(SO_4)_2{\cdot}6H_2O$ in the laboratory frame

The NMR spectrum of ^{39}K ($I = 3/2$) in $K_2Zn(SO_4)_2{\cdot}6H_2O$ single crystals was obtained at a frequency 18.67 MHz. When such crystals are rotated about the crystallographic

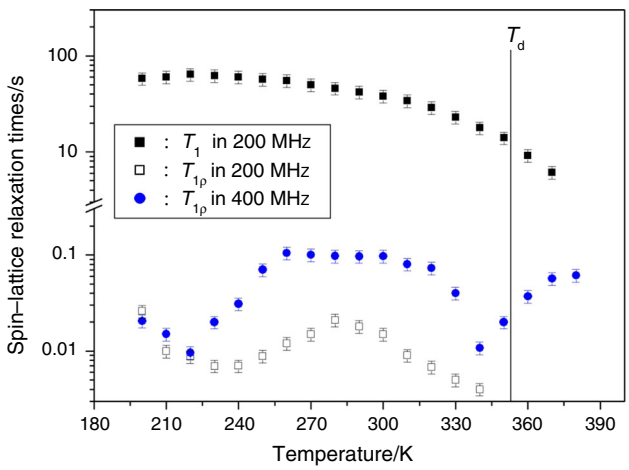

Fig. 4 ^{1}H T_1 and $T_{1\rho}$ in $K_2Zn(SO_4)_2{\cdot}6H_2O$ by static NMR and MAS NMR as a function of temperature

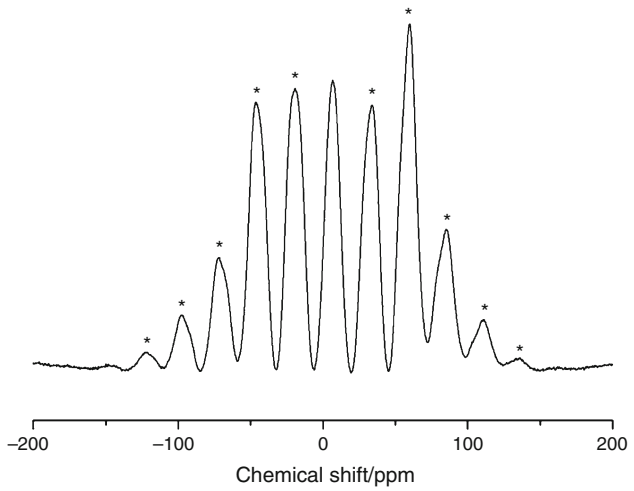

Fig. 5 Chemical shifts of ^{1}H MAS NMR in $K_2Zn(SO_4)_2{\cdot}6H_2O$ at 300 K ($\omega_0/2\pi = 400$ MHz)

axis, crystallographically equivalent nuclei may give rise to three lines in the spectrum: one central line and two satellite lines. The NMR spectrum of ^{39}K consists of two central lines at room temperature, as shown in Fig. 6. The magnitudes of the quadrupole parameters of ^{39}K nuclei are on the order of megahertz; hence, only central lines are usually obtained. The satellite resonance lines for ^{39}K nuclei corresponding to transitions between the levels (+3/2 ↔ 1/2) and (–1/2 ↔ –3/2) are out of the frequency range of the NMR probe. These two K signals are the ^{39}K central NMR lines due to the two inequivalent ^{39}K nuclei, K(1) and K(2). Montgomery and Lingafeller [12] have previously reported that the K nuclei in the crystal structure are crystallographically equivalent. From these results, we are led to believe that two types of magnetically inequivalent K nuclei exist in the unit cell. As was previously reported, the resonance lines of several groups for M nuclei in $M_2Zn(SO_4)_2{\cdot}6H_2O$ (M = Na, K, Rb, and Cs) were caused by magnetically inequivalent but chemically equivalent sites: Na(1) and Na(2) for ^{23}Na nuclei [16], K(1) and K(2) for ^{39}K nuclei, Rb(1) and Rb(2) for ^{87}Rb nuclei [16], and Cs(1) and Cs(2) for ^{133}Cs nuclei [17]. The ^{39}K spectrum consists of two lines displaced to lower frequencies relative to the reference signal, which is the ^{39}K line obtained from an aqueous solution of KBr. The resonance frequencies of the K(1) and K(2) signals are shown as a function of temperature in the inset in Fig. 7. The frequencies of the K(1) and K(2) signals increase slowly with increasing temperature. Above 370 K, the K resonance lines suddenly disappear due to line broadening.

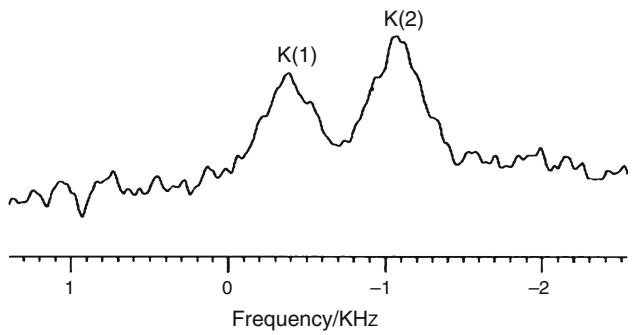

Fig. 6 NMR spectrum of K(1) and K(2) in $K_2Zn(SO_4)_2{\cdot}6H_2O$ single crystals at 300 K

The nuclear magnetization recovery curves of the ^{39}K nuclei were obtained by measuring the nuclear magnetization at several temperatures. The inversion recovery trace for the central resonance line of ^{39}K, with dominant quadrupole relaxation, can be represented by the combination of two exponential functions [14]:

$$[S(\infty) - S(t)]/2S(\infty) = 0.5[\exp(-2W_1 t) + \exp(-2W_2 t)] \quad (2)$$

The temperature dependence of the ^{39}K spin–lattice transition rates W_1 and W_2 was obtained, and W_1 is nearly equal to W_2 over the whole temperature range. If W_1 and W_2 have the same values in the recovery traces of ^{39}K, we can define a relaxation time T_1 as $T_1 = 1/2W_1$. When W_1 is not equal W_2, the constant $5/[2(W_1 + W_2)]$ is introduced instead of T_1; this constant is equal to T_1 when $W_1 = W_2$. We measured the relaxation times of the central lines for K(1) and K(2) with increasing temperature. The trends in the relaxation times for K(1) and K(2) are very similar; their values are consistent within the error range. The temperature dependence of T_1 for ^{39}K nuclei is shown in Fig. 7.

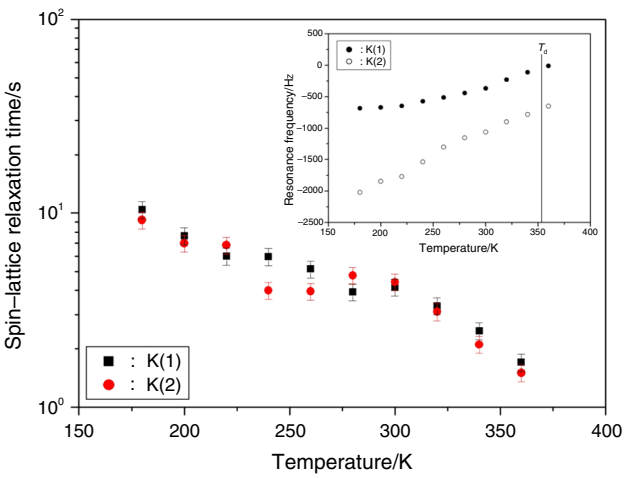

Fig. 7 Spin–lattice relaxation times in the laboratory frame for K(1) and K(2) in $K_2Zn(SO_4)_2{\cdot}6H_2O$ by static NMR as a function of temperature (*inset* resonance frequency of K(1) and K(2) NMR in $K_2Zn(SO_4)_2{\cdot}6H_2O$ as a function of temperature)

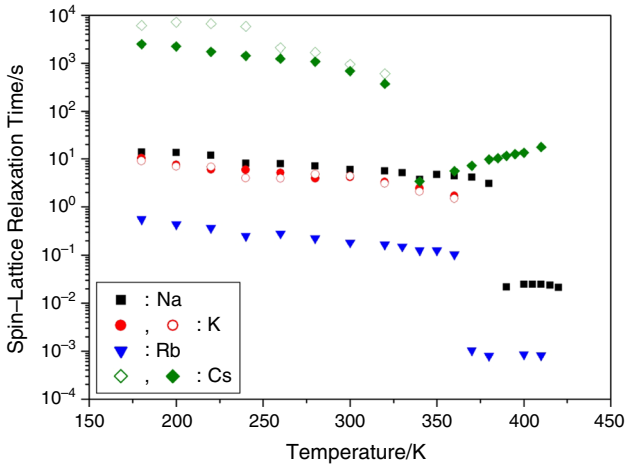

Fig. 8 Spin–lattice relaxation times in the laboratory frame T_1 for M in $M_2Zn(SO_4)_2{\cdot}6H_2O$ (M = Na, K, Rb, and Cs) as a function of temperature

Table 1 Spin–lattice relaxation times/T_1 and electric quadrupole moments/Q in $M_2Zn(SO_4)_2{\cdot}6H_2O$ (M = Na, K, Rb, and Cs)

Nucleus	T_1/s at 300 K	$Q/10^{-30}$ m^2
Na	10	0.14–0.15
K	4	0.11
Rb	0.3	0.13
Cs	1000	−0.003

Conclusions

The thermodynamic properties of $K_2Zn(SO_4)_2{\cdot}6H_2O$ were investigated. The first mass loss occurs near 353 K (T_d), which is interpreted as the onset of partial thermal decomposition. The mass loss is continuous changed from T_d to 440 K; the H_2O content in the crystal decreases with increasing temperature. The phase transitions are restricted to changes in structure only, without any changes in composition [18]. As shown in Fig. 3, the mass loss continues, and it means that thermal decomposition of $K_2Zn(SO_4)_2{\cdot}6H_2O$ crystals takes place continuously via dehydrations. The transformation anomalies at 383 and 410 K are decomposition stage in two consecutive steps. Therefore, the transformation anomalies at 383 and 410 K are not related to structural phase transitions. Near T_d, the relaxation time for the ^{1}H nuclei slowly decreases. This is related to the beginning of the loss of H_2O as observed in the TG results and indicates that the forms of the octahedra of water molecules surrounding Zn^{2+} ions might be disrupted. The disruption of the octahedral is due to proton hopping and breaking of hydrogen bonds.

The experimental results for $K_2Zn(SO_4)_2{\cdot}6H_2O$ were compared with those for $Na_2Zn(SO_4)_2{\cdot}6H_2O$, $Rb_2Zn(SO_4)_2{\cdot}6H_2O$, and $Cs_2Zn(SO_4)_2{\cdot}6H_2O$, as shown in Fig. 8 [16, 17]. The T_1 values for the M nuclei are different owing to differences in the local environments of these ions. The difference between the spin–lattice relaxation times in the laboratory frame of these materials can be attributed to the different electric quadrupole moments (Table 1). This suggests that the differences in the chemical properties of M (=Na, K, Rb, and Cs) are responsible for the variations in the nature of the dehydration in these materials.

Acknowledgements This research was supported by the Basic Science Research program through the National Research Foundation of Korea (NRF) funded by the Ministry of Education, Science, and Technology (2015R1A1A3A04001077).

References

1. Gronvold F, Meisingset KK. Thermodynamic properties and phase transitions of salt hydrates between 270 and 400 K I. $NH_4Al(SO_4)_2{\cdot}12H_2O$, $KAl(SO_4)_2{\cdot}12H_2O$, $Al_2(SO_4)_3{\cdot}17H_2O$, $ZnSO_4{\cdot}7H_2O$, $Na_2SO_4{\cdot}10H_2O$, and $Na_2S_2O_3{\cdot}5H_2O$. J Chem Therm. 1982; 14:1083–98.
2. Lim AR. Study on the phase transitions by nuclear magnetic resonance of α-type $RbAl(SO_4)_2{\cdot}12H_2O$ and β-type $CsAl(SO_4)_2{\cdot}12H_2O$ single crystals. Solid State Nucl Magn Reson. 2009;36:45–51.
3. Jain VK, Venkateswarlu P. On the ^{57}Fe Mossbauer spectra of FeTe and Fe_2Te_3. J Phys C Solid State Phys. 1979;12:865–73.
4. Marinova D, Georgiev M, Stoilova D. Vibrational behavior of matrix-isolated ions in Tutton compounds. II. Infrared spectroscopic study of NH_4^+ and SO_4^{2-} ions included in copper sulfates and selenates. J Mol Struct. 2009;938:179–84.
5. Marinova D, Georgiev M, Stoilova D. Vibrational behavior of matrix-isolated ions in Tutton compounds. I. Infrared spectroscopic study of NH_4^+ and SO_4^{2-} ions included in magnesium sulfates and selenates. J Mol Struct. 2009;929:67–72.
6. Marinova D, Georgiev M, Stoilova D. Vibrational behavior of matrix-isolated ions in Tutton compounds. IV. Infrared spectroscopic study of NH_4^+ and SO_4^{2-} ions included in nickel sulfates and selenates. Cryst Res Technol. 2010;45:637–42.
7. Georgiev M, Marinova D, Stoilova D. Vibrational behavior of matrix-isolated ions in Tutton compounds. III. Infrared spectroscopic study of NH_4^+ and SO_4^{2-} ions included in cobalt sulfates and selenates. Vib Spectrosc. 2010;53:233–8.
8. Riley MJ, Hitchman MA, Mohammed AW. Interpretation of the temperature dependent g values of the $Cu(H_2O)_6^{2+}$ ion in several host lattices using a dynamic vibronic coupling model. J Chem Phys. 1987;87:3766–78.
9. Hoffmann SK, Goslar J, Hilczer W, Augustyniak MA, Marciniak M. Vibronic behavior and electron spin relaxation of Jahn–Teller complex $Cu(H_2O)_6^{2+}$ in $(NH_4)_2Mg(SO_4)_2{\cdot}6H_2O$ single crystal. J Phys Chem A. 1998;102:1697–707.
10. Parthiban S, Anandalakshmi H, Senthilkumar S, Karthikeyan V, Mojumdar SC. Influence of Vo(II) doping on the thermal and optical properties of magnesium rubidium sulfate hexahydrate crystals. J Therm Anal Calorim. 2012;108:881–5.
11. Ganesh G, Ramadoss A, Kannan PS, Subbiahpandi A. Crystal growth, structural, thermal, and dielectric characterization of Tutton salt $(NH_4)_2Fe(SO_4)_2{\cdot}6H_2O$ crystals. J Therm Anal Calorim. 2013;112:547–54.
12. Montgomery H, Lingafelter EC. The crystal structure of Tutton's salts. III. Copper ammonium sulfate hexahydrate. Acta Crystallogr. 1966;20:659–62.

13. SMART and SAINT-Plus v6.22 (2000) Bruker AXS Inc., Madison, Wisconsin, USA.
14. Cowan B. Nuclear Magnetic Resonance and Relaxation. UK: Cambridge University; 1997.
15. Dolinsek J, Arcon D, Zalar B, Pire R, Blinc R, Kind R. Quantum effects in the dynamics of proton glasses. Phys Rev B. 1996;54: R6811–4.
16. Lim AR, Lee JH. ^{23}Na and ^{87}Rb relaxation study of the structural phase transitions in the Tutton salts $Na_2Zn(SO_4)_2{\cdot}6H_2O$ and $Rb_2Zn(SO_4)_2{\cdot}6H_2O$ single crystals. Phys Status Solidi B. 2010; 247:1242–6.
17. Lim AR, Kim SH. Study on structural phase transitions and relaxation processes of $Cs_2Co(SO_4)_2{\cdot}6H_2O$ and $Cs_2Zn(SO_4)_2{\cdot}6H_2O$ crystals. Mater Chem Phys. 2009;117:557–61.
18. Lee KS. Comments concerning "Thermodynamic properties and phase transitions of Tutton salt $(NH_4)_2Co(SO_4)_2{\cdot}6H_2O$ crystals". J Therm Anal Calorim. 2014;115:975–7.